National Aeronautics and
Space Administration
Goddard Space Flight Center
Greenbelt, MD 20771

Reply to Attn of: **Hydrological Sciences Branch, Code 974**

March 2, 2000

TO: Dr. Kenneth H. Bergman
National Aeronautics and Space Administration: Headquarters
NASA Seasonal-to-Interannual Prediction Project (NSIPP) (NRA 98-OES-07)
Code YS
Washington, DC 20546-0001 USA

Dr. Michele Reinecker
National Aeronautics and Space Administration: Headquarters
NASA Seasonal-to-Interannual Prediction Project (NSIPP)
Code 971
Greenbelt, MD 20771 USA

RE: NSIPP Project: *Optimal Land Initialization for Seasonal Climate Predictions,* P. R. Houser (NASA-GSFC Co-PI) and J. S. Famiglietti (U. of Texas Co-PI)

Drs. Bergman and Reinecker,

Enclosed please find a progress report reviewing the progress made in the first year of our NSIPP project "Optimal Land Initialization for Seasonal Climate Predictions" performed under NRA 98-OES-07. This report represents the work completed at GSFC; a separate report will be forwarded from the University of Texas to review their contribution.

We thank you for the opportunity to participate in the NSIPP Project. We have found the first year of this project to be extremely intellectually rewarding, and have found the interaction with other NSIPP project scientists and science team members to be very beneficial. If you have any questions about this report, or need any further information, please do not hesitate to contact us. We thank you for this opportunity to participate in the NSIPP research program, and look forward to ever increasing contributions to it.

Sincerely yours,

Dr. Paul R. Houser
Hydrological Sciences Branch & Data Assimilation Office
NASA Goddard Space Flight Center, Code 974
Greenbelt, MD 20771
301/614-5772 FAX: 301/614-5808
Paul.Houser@gsfc.nasa.gov

Dr. Jeffrey Walker
Hydrological Sciences Branch
NASA Goddard Space Flight Center, Code 974
Greenbelt, MD 20771
301/614-5804 FAX: 301/614-5808
cejpw@land.gsfc.nasa.gov

Optimal Land Initialization for Seasonal Climate Prediction

1 PROJECT OVERVIEW

Accurate initialization of land surface moisture stores in fully-coupled climate systems is critical for *seasonal-to-interannual* climatological and hydrological prediction, because of their regulation of surface water and energy fluxes between the surface and atmosphere over a variety of timescales. Subsurface moisture stores exhibit persistence on *seasonal-to-interannual* timescales; together with external forcing and internal land surface dynamics, this persistence has important implications for the extended prediction of climatic and hydrologic extremes. Because these are integrated states, errors in land surface forcing and parameterization accumulate in these stores, which leads to incorrect surface water and energy partitioning. However, many innovative new land surface observations are becoming available that may provide the additional information necessary to constrain the initialization of land surface states critical for *seasonal-to-interannual* prediction. These constraints can be imposed in two ways. Firstly, by forcing the land surface primarily by observations (such as precipitation and radiation), the often severe numerical weather prediction land surface forcing biases can be avoided. Secondly, by employing innovative land surface data assimilation techniques, observations of land surface storages (such as soil moisture) can be used to constrain unrealistic simulated storages.

We are pursuing a two-tiered approach of providing an accurate initialization of land surface moisture stores for long-term climate prediction. The first tier uses improved land surface forcing to evolve improved land states. This first tier is being spearheaded by Professor Famiglietti and his student, Aaron Berg, at the University of Texas. The second tier, which further constrains the initial states using remotely sensed soil moisture using data assimilation methods, is the responsibility of Dr. Houser and Dr. Walker at NASA's Goddard Space Flight Center. Dr. Walker joined the tier two effort in July 1999. Dr. Walker is uniquely qualified for this project as he has extensive knowledge of land surface observation, modeling, and Kalman filtering techniques. We have also purchased a state-of-the-art Linux-based 2-processor Alpha computer and 400gb of disk storage in support of both tiers of this project. This report outlines the progress made by Dr. Houser and Dr. Walker on the second tier, and interactions with the University of Texas concerning the first tier during the period July 1999 to February 2000. The progress made by Professor Famiglietti will be the subject of a separate report submitted via the University of Texas.

2 PROGRESS ON OFF-LINE CATCHMENT MODELING

The catchment-based land surface model (LSM) of Koster *et al.* [2000] has developed substantially over the past months, as a direct result of our simulations and evaluation of its predicted soil moisture. The catchment-based LSM predicts water deficit, root zone excess and surface excess as the soil moisture prognostic variables for given watershed areas, rather than soil moisture directly. We must derive volumetric soil moisture analytically from the model water excess and deficit states for validation with observations and for use in Kalman filter development. In this process we found that the LSM was forecasting negative soil moisture for some parts of the model domain. After pointing this problem out to Dr. Koster, the LSM was modified and appropriate checks put in place to ensure that the resulting soil moisture remained within physical bounds. However, these modifications to the model physics resulted in the surface soil moisture being generally greater than the deep soil moisture, which is unrealistic. Additional changes were made by Dr. Koster, such that the LSM now forecasts expected soil moisture variation with depth, which lies within physical bounds.

3 SOIL MOISTURE COMPARISON: REMOTE SENSING VERSUS LSM

A comparison of near-surface soil moisture estimates from the catchment-based LSM and Scanning Multi-channel Microwave Radiometer (SMMR) remote sensing observations are given in Figures 1 and 2. While Figure 1 shows that there are some consistent patterns between the spatial soil moisture plots from the LSM and the SMMR data, there are some significant discrepancies. This is to be expected, as the soil moisture forecasts from the LSM are subject to the spin-up initialization states and the atmospheric forcing data, both of which may be erroneous. Moreover, soil moisture forecasts from the LSM may be subject to errors in the model physics. If however there was already a good agreement between the SMMR soil moisture observations and the LSM soil moisture forecasts, then it would be pointless for us to continue with either tier of this project.

The time series comparisons in Figure 2 show that the catchment-based LSM and the SMMR soil moisture observations track each other consistently in some locations, but with a spatially varying bias. Such results are indicative of initialization errors in these locations. However, the exact relationship between the two sources of soil moisture is less clear in other locations, perhaps as a result of errors in atmospheric forcing. Moreover, the comparison with ground measured soil moisture (average of 6 point measurements) is poor for both the LSM and the SMMR soil moisture observations, even when taking into account the large error bars on the observations. While the extremely poor comparison of SMMR data with the ground measurements during the winter months may be explained by the presence of snow or frozen soil, the poor comparison with the LSM is more difficult to explain. However, it has been found that changing the topographical parameters in the LSM yields a greater wet-up of the soil during the winter months. This comparison shows that our future assimilation work may have great potential to improve the current model simulations, but that we may be greatly limited by observation errors in the remote sensing data.

4 PROGRESS IN SOIL MOISTURE ASSIMILATION

The Kalman filter assimilation scheme is a linearized statistical scheme that provides a statistically optimal update of the system states based on the relative magnitudes of the covariances of both the model system state estimate and the observations. The principal advantage of this approach is that the Kalman filter provides a framework within which the entire system is modified, with covariances representing the reliability of the observations and model prediction.

4.1 The (Extended) Kalman Filter

The Kalman filter algorithm [Kalman, 1960] tracks the conditional mean of a statistically optimal estimate of a state vector $\mathbf{X}$, through a series of forecasting and update steps. To apply the Kalman filter, the equations for evolving the system states must be written in the linear state space formulation of (1). When these equations are non-linear, the Kalman filter is called the

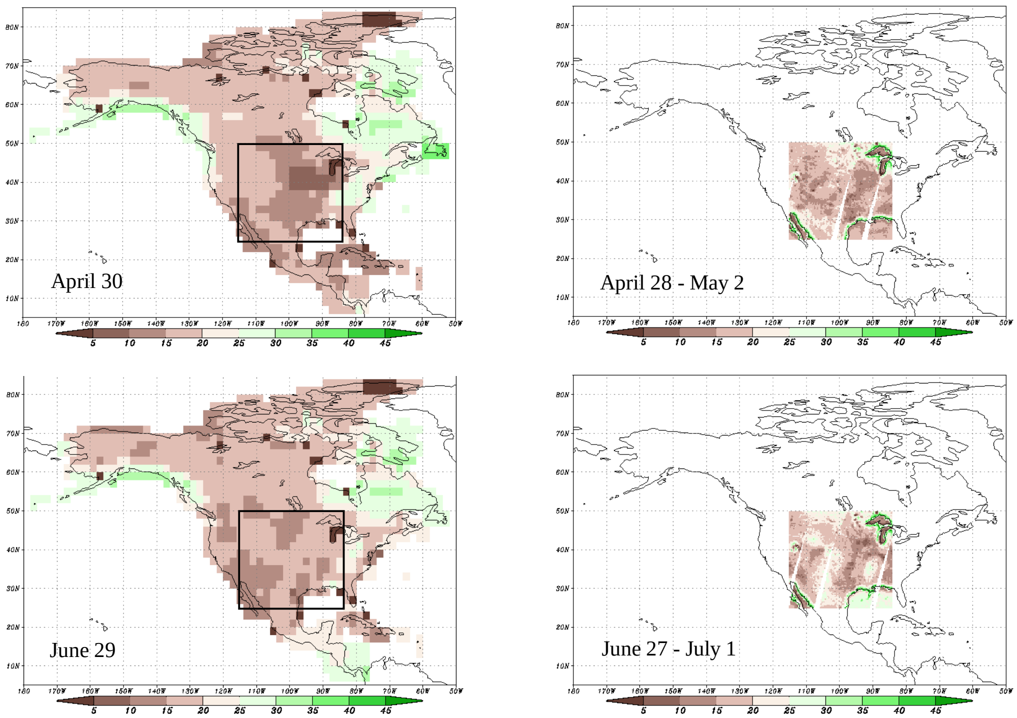

Figure 1: Spatial comparison of near-surface soil moisture from the catchment-based LSM (left) with remotely sensed estimates from the SMMR satellite (right) in 1987.

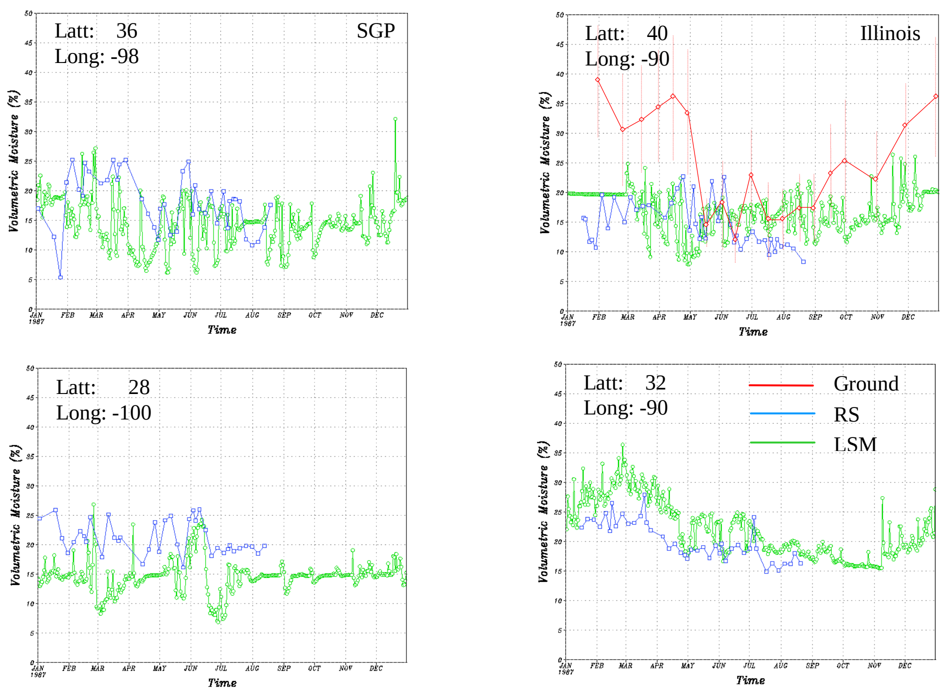

Figure 2: Time series comparison of near-surface soil moisture from the catchment-based LSM with remotely sensed estimates from the SMMR satellite and ground measurements in 1987 for a $2° \times 2°$ grid cell centered on the latitude and longitude given.

extended Kalman filter, and is an approximation of the non-linear system that is based on first-order linearization. The forecasting equations are [Bras and Rodriguez-Iturbe, 1985]

$$\hat{\mathbf{X}}^{n+1/n} = \mathbf{A}^n \cdot \hat{\mathbf{X}}^{n/n} + \mathbf{U}^n + \left(\mathbf{w}^n\right) \qquad (1)$$

$$\acute{\mathbf{O}}_{\mathrm{x}}^{n+1/n} = \mathbf{A}^n \cdot \acute{\mathbf{O}}_{\mathrm{x}}^{n/n} \cdot \mathbf{A}^{n^{\mathrm{T}}} + \mathbf{Q}^n \qquad (2),$$

where **A** is the state propagation matrix relating the system states at times n+1 and n, **U** is a vector of forcing, **w** is the model error, $\acute{\mathbf{O}}_{\mathrm{x}}$ is the covariance matrix of the system states and **Q** is the covariance matrix of the system noise (model error), defined as E[$\mathbf{w}\cdot\mathbf{w}^{\mathrm{T}}$]. The notation n+1/n refers to the system state estimate at time n+1 from a forecasting step, and n/n refers to the system state estimate from either a forecasting or updating step at time n.

For the update step, the observation vector **Z** must be linearly related to the system state vector **X** through the transformation matrix **H**.

$$\mathbf{Z} = \mathbf{H} \cdot \hat{\mathbf{X}} + \mathbf{Y} + (\mathbf{v}) \qquad (3),$$

where **Y** contains the state independent terms and **v** accounts for observation and linearization errors.

Updating of the best estimate of the system state vector $\hat{\mathbf{X}}$ by the observation vector **Z** is performed by means of Bayesian statistics. The system state vector and associated covariances are updated by the expressions [Bras and Rodriguez-Iturbe, 1985]

$$\hat{\mathbf{X}}^{n+1/n+1} = \hat{\mathbf{X}}^{n+1/n} + \mathbf{K}^{n+1}\left(\mathbf{Z}^{n+1} - \left(\mathbf{H}^{n+1} \cdot \hat{\mathbf{X}}^{n+1/n} + \mathbf{Y}^{n+1}\right)\right) \qquad (4)$$

$$\acute{\mathbf{O}}_{\mathrm{x}}^{n+1/n+1} = \left(\mathbf{I} - \mathbf{K}^{n+1} \cdot \mathbf{H}^{n+1}\right) \cdot \acute{\mathbf{O}}_{\mathrm{x}}^{n+1/n} \cdot \left(\mathbf{I} - \mathbf{K}^{n+1} \cdot \mathbf{H}^{n+1}\right)^{\mathrm{T}} + \mathbf{K}^{n+1} \cdot \mathbf{R}^{n+1} \cdot \mathbf{K}^{n+1^{\mathrm{T}}} \qquad (5),$$

where **I** is the identity matrix. The Kalman gain matrix $\mathbf{K}^{n+1}$ weights the observations against the model forecast. Its' weighting is determined by the relative magnitudes of model uncertainty embodied in $\acute{\mathbf{O}}_{\mathrm{x}}^{n+1/n}$ with respect to the observation covariances $\mathbf{R}^{n+1}$, defined as E[$\mathbf{v}\cdot\mathbf{v}^{\mathrm{T}}$]. The Kalman gain is given by

$$\mathbf{K}^{n+1} = \acute{\mathbf{O}}_{\mathrm{x}}^{n+1/n} \cdot \mathbf{H}^{n+1^{\mathrm{T}}} \cdot \left(\mathbf{R}^{n+1} + \mathbf{H}^{n+1} \cdot \acute{\mathbf{O}}_{\mathrm{x}}^{n+1/n} \cdot \mathbf{H}^{n+1^{\mathrm{T}}}\right)^{-1} \qquad (6).$$

Given the initial state vector $\hat{\mathbf{X}}^{0/0}$ with covariance matrix $\acute{\mathbf{O}}_{\mathrm{x}}^{0/0}$, the system states and covariances are forecast (denoted by the time superscript n+1/n) using (1) and (2) respectively. When an observation becomes available, an update of the system states and covariances is made (denoted by the time superscript n+1/n+1) using (4) and (5) respectively.

4.2 The Land Surface Model

The LSM used in this project is the catchment-based LSM of Koster *et al.* [2000], illustrated schematically in Figure 3. The catchment-based LSM soil moisture prognostic variable forecasting equations are given by

$$srfexc^{n+1} = srfexc^{n} - srflow + i - es \qquad 0 \le srfmc \le poros \qquad (7)$$

$$rzexc^{n+1} = rzexc^{n} + srflow - rzflow - ev \qquad -rzeq \le rzexc \le (rzmax - rzeq) \qquad (8)$$

$$catdef^{\,n+1} = catdef^{\,n} - rzflow + baseflow + et \qquad 0 \le catdef \le cdmax \qquad (9),$$

where *srfexc* is the surface excess, *rzexc* is the root zone excess, *catdef* is the catchment deficit, *srfmc=f*(*srfexc*,*rzexc*,*catdef*) is the near-surface soil moisture, *poros* is the soil porosity, *rzeq* is the soil moisture in the root zone at equilibrium based on the catchment deficit, *rzmax* is the maximum soil moisture storage in the root zone, *cdmax* is the maximum catchment deficit, and the superscript *n* is the time tag. The redistribution between the surface excess and root zone excess is given by *srflow=f*(*srfexc*,*rzexc*), and between the root zone excess and catchment deficit is given by *rzflow=f*(*rzexc*,*catdef*). The baseflow is given by *baseflow=f*(*catdef*), the soil infiltration is given by *i=f*(*srfexc*,*rzexc*,*catdef*), the bare soil evaporation is given by *es=f*(*srfexc*,*rzexc*,*catdef*), the transpiration is given by *ev=f*(*srfexc*,*rzexc*,*catdef*), and the evapotranspiration is given by *et=f*(*srfexc*,*rzexc*,*catdef*).

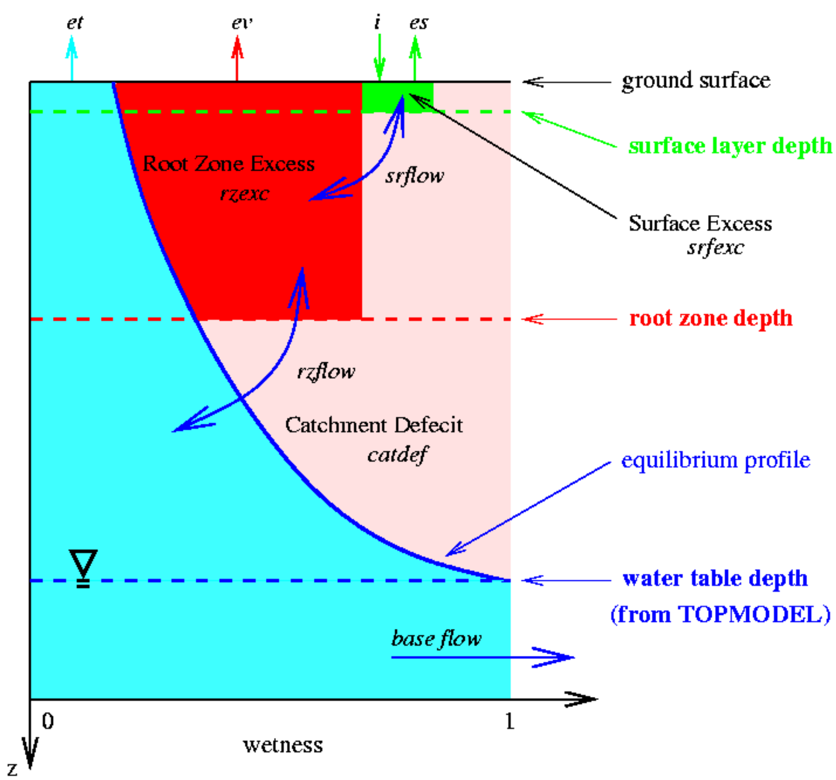

Figure 3: Schematic of the catchment-based LSM soil moisture prognostics.

Table 1: Minimum values for standard deviations of the forecast model error covariance matrix **Q** (mm/min).

srfexc	0.0025
rzexc	0.025
catdef	0.25

4.3 Application of the Kalman Filter to the Catchment-Based Land Surface Model

In this project, we have used a one-dimensional Kalman filter for updating the soil moisture prognostic variables of the catchment-based LSM. A one-dimensional Kalman-filter was used because of its computational efficiency and the fact that horizontal correlation between soil moisture prognostic variables of adjacent catchments at the scales of interest to NSIPP is likely only through the large-scale correlation of atmospheric forcing. Moreover, all calculations for soil moisture in the catchment-based LSM are performed independent of the soil moisture in adjacent catchments.

4.3.1 Covariance Forecasting

Forecasting of the soil moisture covariance matrix using Kalman filter theory requires a linear forecast model. However, forecasting of the soil moisture prognostic variables (surface excess, root zone excess and catchment deficit) in the catchment-based LSM is non-linear. Hence, forecasting of the soil moisture prognostic variables covariance matrix was achieved through linearization of the soil moisture forecasting equations. The linearization was performed by a first order Taylor series expansion of the non-linear forecasting equations (7-9). Using this approach, the covariance forecasting matrix is given by

$$\mathbf{A} = \begin{bmatrix} \dfrac{\partial srfexc^{n+1}}{\partial srfexc^{n}} & \dfrac{\partial srfexc^{n+1}}{\partial rzexc^{n}} & \dfrac{\partial srfexc^{n+1}}{\partial catdef^{\,n}} \\ \dfrac{\partial rzexc^{n+1}}{\partial srfexc^{n}} & \dfrac{\partial rzexc^{n+1}}{\partial rzexc^{n}} & \dfrac{\partial rzexc^{n+1}}{\partial catdef^{\,n}} \\ \dfrac{\partial catdef^{\,n+1}}{\partial srfexc^{n}} & \dfrac{\partial catdef^{\,n+1}}{\partial rzexc^{n}} & \dfrac{\partial catdef^{\,n+1}}{\partial catdef^{\,n}} \end{bmatrix} \qquad (10).$$

For the initial covariance matrix, diagonal terms were specified to have a standard deviation of the maximum difference between the initial prognostic state value and the upper and lower limits. This represents a large uncertainty in the initial soil moisture prognostic state values and the fact that the true initial soil moisture prognostic variable could in fact be anywhere within the possible range. Off diagonal terms were specified to be zero initially, suggesting a zero correlation between the three soil moisture prognostic variables. The diagonal terms of the forecast model error covariance matrix **Q** were taken as the predefined values given in Table 1, with the off diagonal terms taken to be zero.

4.3.2 Kalman Filter Observation Equation

In order to perform an update of the soil moisture prognostic variables with the Kalman filter, the observation (near-surface soil moisture) must be linearly related to the soil moisture

Table 2: Uniform soil properties specified for North America.

saturated surface hydraulic conductivity	2.2×10^{-3} m s^{-1}
transmittivity decay factor	3.26 m^{-1}
saturated soil matric potential	–0.281 m
Clapp and Hornberger (1978) *b*	4
root zone depth	1 m
wilting point wetness	0.148/*poros*

prognostic variables. In the catchment-based LSM, the soil moisture prognostic variables are the surface excess, root zone excess, and catchment deficit, which are related to the observed volumetric soil moisture of the surface layer through a complicated non-linear function

$$srfmc = f_w(rzexc, catdef) \times poros + \frac{srfexc}{z_1} \quad (11),$$

where z_1 is the surface layer thickness (2 cm). Using a first order Taylor series expansion of the non-linear function f_w in the surface soil moisture equation

$$\begin{aligned}[srfmc] = &\begin{bmatrix} \frac{1}{z_1} & \frac{\partial f_w}{\partial rzexc} poros & \frac{\partial f_w}{\partial catdef} poros \end{bmatrix} \begin{bmatrix} srfexc \\ rzexc \\ catdef \end{bmatrix} + \\ &\left[poros\left(f_w^* - \frac{\partial f_w}{\partial rzexc} rzexc^* - \frac{\partial f_w}{\partial catdef} catdef^* \right)\right] \end{aligned} \quad (12),$$

where the * refers to prognostic variable values about which the Taylor series expansion is evaluated.

4.4 Numerical Experiments

A set of numerical experiments have been undertaken for the entire North America, in order to illustrate the effectiveness of the assimilation scheme in providing a more accurate estimate of the soil moisture storage throughout the entire soil profile. Moreover, the corresponding influence on the water balance components, namely evapotranspiration and runoff, has been illustrated.

4.4.1 Model Input Data

In this experiment, atmospheric forcing data and soil and vegetation properties from the first ISLSCP initiative [Sellers *et al.*, 1996] have been used as model input for the year 1987. Such data includes: air temperature and humidity at two meters, surface wind speed and atmospheric pressure, precipitation, downward solar and longwave radiation, greenness, leaf area index, surface roughness length, surface snow free albedo, canopy height, vegetation class, soil porosity, soil depth and soil texture. Soil properties not defined by ISLSCP were taken to be uniform across North America with the values given in Table 2. Topographic parameters were derived from a 30-arc-second (≈1 km) digital elevation model of North America from the USGS

EROS Data Center [Ducharne *et al*., 2000]. The initial model states for 1987 in each of the 5018 catchments used to model the entire North America were determined by driving the model to equilibrium at the beginning of 1987 to avoid a non-equilibrated spin-up signal.

4.4.2 Observation and Evaluation Data

Using the LSM of Koster *et al*. [2000], the initial conditions from spin-up, and the model input data described above, the temporal and spatial variation of soil moisture across North America was forecast for 1987. The forecasts of near-surface soil moisture were output once every 3 days to represent the near-surface soil moisture measurements from remote sensors. In addition to soil moisture (Figures 4b and 5b), the land surface model provided estimates of evapotranspiration (Figure 6b) and runoff (Figure 7b) for each of the catchments. This simulation provided the “true” soil moisture and water balance data for comparison with degraded simulations. Moreover, it allowed evaluation of the effectiveness of assimilating near-surface soil moisture data for improving the LSM forecast of soil moisture and water budget components, when initialized with poor soil moisture initial conditions.

4.4.3 Degraded Simulation

In the degraded simulation, the initial conditions for the soil moisture prognostic variables from the spin-up were set to arbitrarily wet values, uniformly across the entire North America. The LSM was then forced with the same atmospheric data as in the previous simulation. The effects of this degradation on the soil moisture forecasts are obvious from Figures 4a and 5a. Figure 5a shows that even after twelve months there was still significant errors in the soil moisture states, particularly in the mid to high latitudes where evapotranspiration rates are low. The soil moisture in low latitudes has merged towards the “truth” as a result of spin-up in the LSM towards the equilibrium states evolving more quickly in the regions of higher evapotranspiration. The effect of a wet initial condition on evapotranspiration and runoff can be seen in Figures 6a and 7a respectively, where both are over-estimated.

4.4.4 Degraded Simulation With Assimilation

The final simulation was to assimilate the near-surface “observations” from the “truth” simulation into the degraded simulation once every 3 days. The effect of assimilation on the soil moisture forecasts can be seen in Figures 4c and 5c. These results show that after only 1 month of assimilation, the “true” soil moisture has been retrieved for the majority of North America, while after 12 months of assimilation there are only a few catchments remaining where the “true” soil moisture has not been retrieved for the entire soil profile. Moreover, the forecast of evapotranspiration (Figure 6c) and runoff (Figure 7c) show a close agreement with the “truth”.

5 NEAR-TERM PLANS AND MILESTONES

- Identify why the correct soil moisture is retrieved more quickly for some catchments compared to others. We believe there may be a decoupling of soil moisture reservoirs with depth that may cause longer retrieval times. This may be due to catchment characteristics or climate conditions for which we have no control, or it may be linked to problems in the observation operator or assimilation algorithm which we can identify and improve.

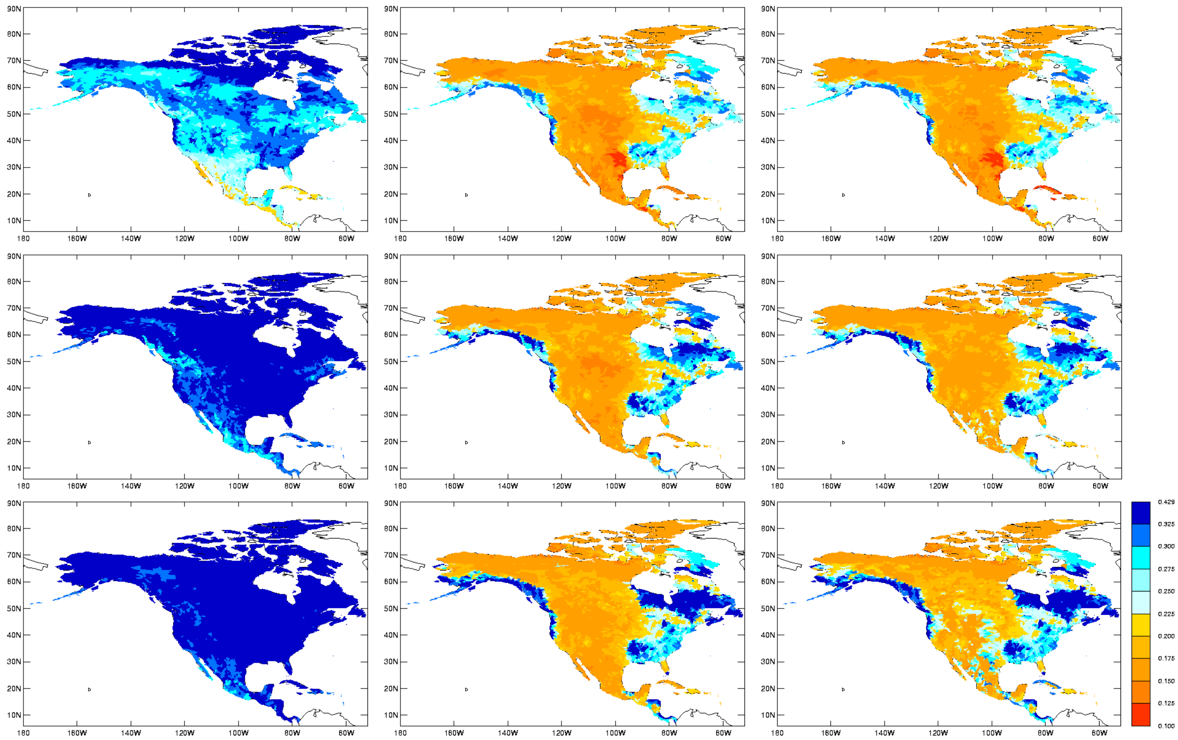

a) b) c)

Figure 4: Comparison of soil moisture (v/v) on 30 January 1987 in near-surface (top row), root zone (middle row) and entire profile (bottom row) from: a) simulation with degraded initial conditions for soil moisture; b) simulation with spin-up initial conditions ("truth"); and c) degraded simulation with assimilation of near-surface soil moisture from the "truth" once every 3 days.

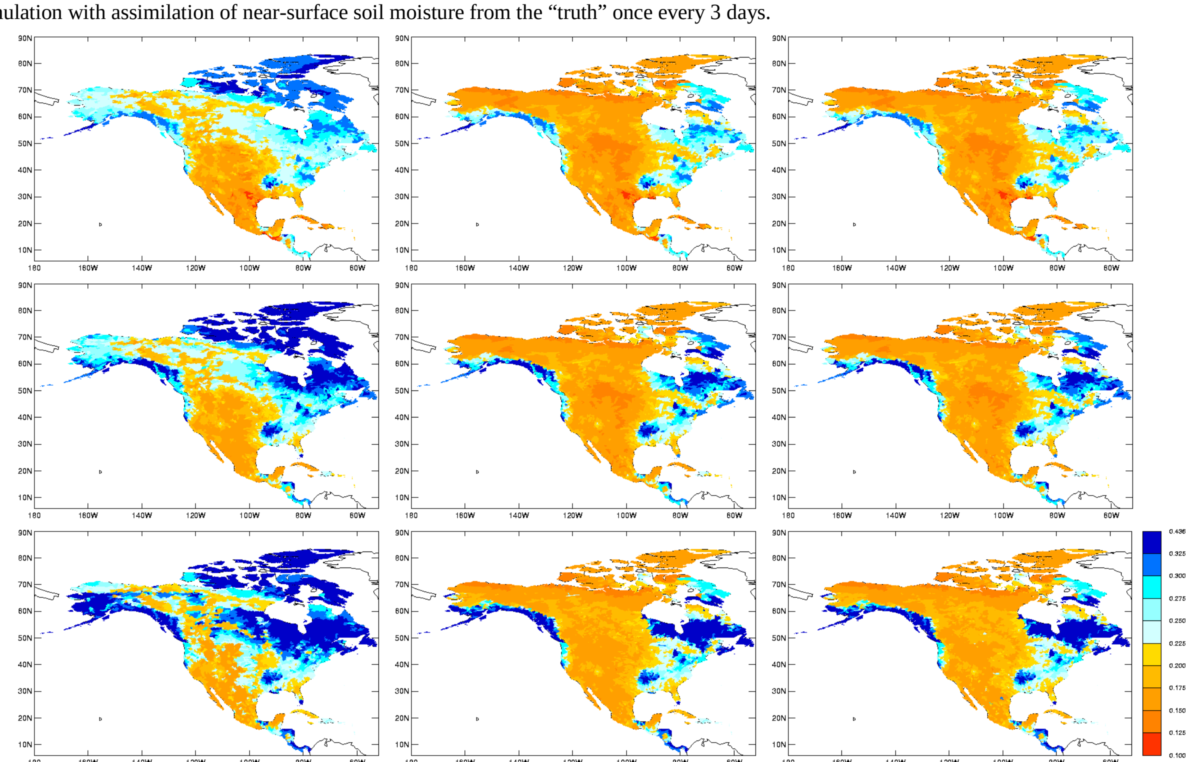

a) b) c)

Figure 5: Comparison of soil moisture (v/v) on 29 December 1987 in near-surface (top row), root zone (middle row) and entire profile (bottom row) from: a) simulation with degraded initial conditions for soil moisture; b) simulation with spin-up initial conditions ("truth"); and c) degraded simulation with assimilation of near-surface soil moisture from the "truth" once every 3 days.

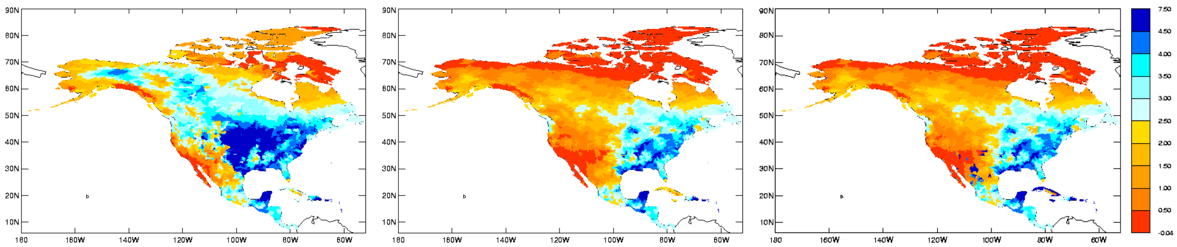

a) b) c)

Figure 6: Comparison of monthly average evapotranspiration (mm/d) for July 1987 from: a) simulation with degraded initial conditions for soil moisture; b) simulation with spin-up initial conditions ("truth"); and c) degraded simulation with assimilation of near-surface soil moisture from the "truth" once every 3 days.

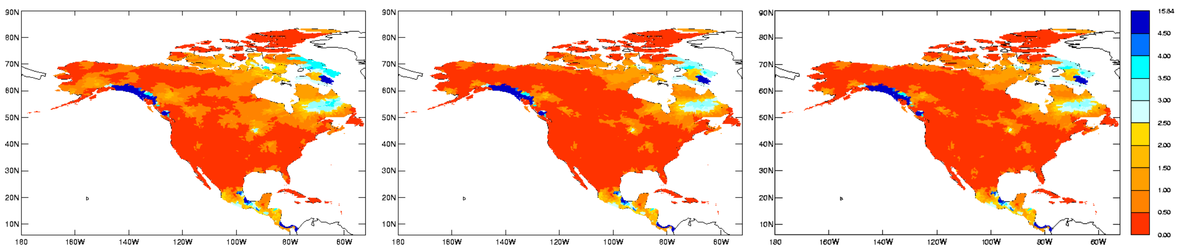

a) b) c)

Figure 7: Comparison of monthly average runoff (mm/d) for July 1987 from: a) simulation with degraded initial conditions for soil moisture; b) simulation with spin-up initial conditions ("truth"); and c) degraded simulation with assimilation of near-surface soil moisture from the "truth" once every 3 days.

• Identify the maximum level of error which surface observations can have before the assimilation is no longer useful. This will help us to avoid using observations with too much error, and will give guidance to future observation platform development.

• Evaluate assimilation performance when error is present in land model forcing and/or parameters.

• Identify the minimum frequency of surface observations before there is a significant degradation of the assimilation results.

• Assimilate Dr. Owe's near-surface soil moisture data over North America and evaluate. Based on the comparisons shown above, we have a great concern about the quality of these observations. The success of out tier-two assimilation approach is entirely dependent on the provision of information from the observations; if there is no information in the observations, then even the best assimilation algorithm is useless. Therefore, we plan to work more closely with Dr. Owe in the near future to push the reliability of his approach forward. We would like to see him utilize a more robust retrieval of soil moisture that does not rely on site-by-site retrieval model calibration, but rather on observed land surface characteristics. We would also like to see him develop robust and independent estimates of observation error for optimizing the assimilation approaches we use. The theory of microwave soil moisture remote sensing is sound, and we believe that there is information in the SMMR observations, so we would like to continue to pursue this approach. However, if near-term progress is not made, we will likely need to use more recent passive microwave observations (from TRMM and AMSR) in place of SMMR, or switch directions and look into alternate sources of soil moisture information (such as from infrared and NDVI), or switch to alternate surface assimilation states (such as temperature).

- Participate in the LDAS project for the purpose of providing near-real time initializations for NSIPP seasonal predictions. We would like to include the catchment model and our assimilation methods in the LDAS system in the near term. The mosaic model is already being used in LDAS, so we may also explore the use of its fields in seasonal-to-interannual initialization.

- Collaborate with the University of Texas on the tier-one initialization approaches. We have already hosted one visit by Mr. Berg to work with Dr. Walker on transferring the ECMWF forcing fields to the NSIPP catchment space. Dr. Walker will be visiting Texas in Mid-March, and Mr. Berg will visit GSFC again this summer for an extended period to strengthen this collaboration. Furthermore, we have arranged for our University of Texas partners to use our computer facilities in support of this work. We believe that having joint access to the forcing data and programs on a common platform will help us to advance our work more quickly. We would like to see the University of Texas have both the ECMWF and NCEP reanalysis forcing in place for use in the catchment model by summer 2000, and for them to make significant progress on bias correcting this forcing using observations by the Fall of 2000. Further, we would like to collaborate with them on runoff routing, and forcing and initialization sensitivity studies in both coupled and off-line modes. In 2001, we envision closer collaboration on using alternate assimilation data in the system, including GRACE.

- Move towards a global implementation of the assimilation. This will require globalization of both the catchment model and the remote sensed soil moisture data being developed by Dr. Owe, both of which are both beyond the scope of our project and are out of our control.

- Develop a set of global soil moisture initialization states for the start of each month from 1978 to 1994.

6 REFERENCES

Bras, R. L., and Rodriguez-Iturbe, I., 1985. *Random Functions and Hydrology*. Addison Wesley, Reading, Massachusetts, USA, 559pp.

Ducharne, A., Koster, R. D., Suarez, M. J., Stieglitz, M., and Kumar, P., 2000. A Catchment-Based Approach to Modelling Land Surface Processes. Part 2: Parameter Estimation and Model Demonstration. *J. Geophys. Res.*, submitted.

Kalman, R. E., 1960. A New Approach to Linear Filtering and Prediction Problems. *Trans. ASME, Ser. D, J. Basic Eng.*, **82**: 35-45.

Koster, R. D., Suarez, M. J., Ducharne, A., Stieglitz, M., and Kumar, P., 2000. A Catchment-Based Approach to Modeling Land Surface Processes in a GCM. Part 1: Model Structure. *J. Geophys. Res.*, submitted.

Sellers, P., Meeson, B. W., Closs, J., Collatz, J., Corprew, F., Dazlich, D., Hall, F. G., Kerr, Y., Koster, R., Los, S., Mitchell, K., McManus, J., Myers, D., Sun, K. J, and Try, P., 1996. The ISLSCP Initiative I Global Data Sets: Surface Boundary Conditions and Atmospheric Forcings for Land-Atmosphere Studies. *Bull. Am. Met. Soc.*